Salirasib (farnesyl thiosalicylic acid) for brain tumor treatment: a convection-enhanced drug delivery study in rats

Liat Goldberg,[1] Aharon Ocherashvilli,[2] Dianne Daniels,[2] David Last,[2] Zvi R. Cohen,[3] Gregory Tamar,[2] Yoel Kloog,[1] and Yael Mardor[2]

[1]Department of Neurobiology, The George S. Wise Faculty of Life Sciences, Tel-Aviv University, Tel Aviv, Israel and [2]The Advanced Technology Center and [3]Neurosurgery Department, Sheba Medical Center, Tel-Hashomer, Israel

Abstract

Our aim was to assess the ability of convection-enhanced drug delivery (CED), a novel approach of direct delivery of drugs into brain tissue and brain tumors, to treat brain tumors using salirasib (farsnesyl thiosalicylic acid). CED was achieved by continuous infusion of drugs via intracranial catheters, thus enabling convective distribution of high drug concentrations over large volumes while avoiding systemic toxicity. Several phase II/III CED-based trials are currently in progress but have yet to overcome two major pitfalls of this methodology (the difficulty in attaining efficient CED and the significant nonspecific neurotoxicity caused by high drug doses in the brain). In this study, we addressed both issues by employing our previously described novel CED imaging and increased efficiency methodologies to exclusively target the activated form of the Ras oncogene in a 9L gliosarcoma rat model. The drug we used was salirasib, a highly specific Ras inhibitor shown to exert its suppressive effects on growth and migration of proliferating tumor cells in *in vitro* and *in vivo* models, including human glioblastoma, without affecting normal tissues. The results show a significant decrease in tumor growth rate in salirasib-treated rats relative to vehicle-treated rats as well as a significant correlation between CED efficacy and tumor growth rate with no observed toxicity despite drug concentrations an order of magnitude higher than previously detected in the brain. The results show that CED of salirasib is efficient and nontoxic for the treatment of glioblastoma in a rat model, thus suggesting that it may be considered for clinical application. [Mol Cancer Ther 2008;7(11):3609–16]

Introduction

Fluid convection (bulk flow), which occurs in the brain interstitial fluid under normal conditions (1), in cases of vasogenic edema (2), and after infusion of solutions directly into the brain parenchyma (3), is a promising technique for the distribution of solutions into brain tissue. The fluid convection established by maintenance of a pressure gradient during interstitial infusion has been shown to greatly enhance the distribution of various molecules in the brain (4, 5). Those studies showed the ability of fluid convection to obtain *in situ* drug concentrations several orders of magnitude greater than those achieved by systemic administration over large volumes of the brain at various time intervals. The concentration profile obtained with convection-enhanced drug delivery (CED) is relatively flat up to the flow front, providing control over undesired toxicity (6).

Application of CED to brain pathology is an emerging field. Most of the studies carried out thus far have focused on the treatment of brain tumors. Our group recently conducted a phase I/II clinical trial in which 15 patients with recurrent glioblastoma multiforme received a total of 20 cycles of intratumoral CED of Taxol with a significant antitumor response rate of 73% (7). In a phase II clinical trial, in which patients were treated by CED of Tf-CRM107 (a conjugate protein of diphtheria toxin with a point mutation linked by a thioester bond to human transferrin), the response rate was 35% (8). Clinical trials have also been conducted with other drugs, such as TP-38 (9) and interleukin-4 (38-37)-PE38KDEL (10), which provided evidence of some clinical activity, and with interleukin-13-PE38QQR (11), which yielded no definite conclusions with regard to efficacy.

In a recent study aimed at integrating drugs into the CED model, we showed that the readily available magnetic resonance imaging (MRI) contrast agent Gd-DTPA could be used as a surrogate marker for immediate assessment of convection efficiency and infusate distribution simply by being mixed with the infusate before infusion (12). The cytotoxic response of brain tissue to therapeutic agents infused via CED could be assessed at an early stage by means of subsequent T_2-weighted and diffusion-weighted MRI. Our data suggested, moreover, that drug distribution can be significantly improved by increasing the infusate viscosity where optimal infusate distribution was achieved with 10% sucrose (12).

Received 5/21/08; revised 8/11/08; accepted 8/15/08.

Grant support: Wolfson Foundation and the Prajs-Drimmer Institute for the Development of Anti-Degenerative Disease Drugs.

The costs of publication of this article were defrayed in part by the payment of page charges. This article must therefore be hereby marked *advertisement* in accordance with 18 U.S.C. Section 1734 solely to indicate this fact.

Note: Y. Kloog is the incumbent of the Jack H. Skirball Chair in Applied Neurobiology.

Requests for reprints: Yoel Kloog, Department of Neurobiochemistry, The George S. Wise Faculty of Life Sciences, Tel-Aviv University, 69978 Tel Aviv, Israel. Phone: 972-3-640-9699; Fax: 972-3-640-7643; E-mail: kloog@post.tau.ac.il

doi:10.1158/1535-7163.MCT-08-0488

At least some nonspecific neurotoxicity was observed in all the drug models tested. This ongoing problem led us to search for novel drugs that show potential antitumor activity with minimal nonspecific toxicity. A suitable candidate for this purpose might be the Ras inhibitor, farsnesyl thiosalicylic acid (salirasib). Ras proteins comprise a family of small GTPases that act as key regulators of cell signaling pathways governing cell proliferation, differentiation (13), migration (14–16), survival, and death (17). On mitogenic stimulation, these proteins switch from the nonactivated, GDP-bound form to the activated, GTP-bound form, and their activity depends on their proper membrane anchorage (18). Accordingly, salirasib was designed to mimic the farnesyl cysteine moiety of the carboxyl terminus of Ras shown to be crucial for such anchorage. By competing with Ras on membrane anchorage sites, salirasib causes dislodgement and rapid degradation of Ras (19).

Salirasib has been shown to be effective against human glioma *in vitro* (16, 20, 21). Inoculation of human gliomas in animal models is usually done in nude mice, which are too small for convection experiments. Therefore, in the present study, we treated 9L-tumor-bearing rats with a salirasib-based infusate, which we have prepared for CED use by adding Gd-DTPA for real-time imaging of the extent of CED and 10% sucrose to increase viscosity. A control group was treated with a similar infusate without the drug. We found that, relative to the control, a single dose of salirasib caused a marked decrease in tumor growth rate with no apparent toxicity. In addition, a clear and significant correlation was found between tumor growth rate and convection efficiency in the salirasib-treated group only.

These promising results, showing the induction of significant antitumor effects without the nonspecific neurotoxicity seen with most chemotherapeutic agents, suggest that salirasib can be considered as a potential therapy for glioblastoma.

Materials and Methods

Cell Culture Procedures

9L gliosarcoma cells were maintained at 37°C and 5% CO_2 in DMEM enriched with 10% FCS and penicillin/streptomycin 1% and were subcultured twice a week. Cells were plated at a density of 5,000 per well in 24-well plates for direct cell counts or at 1×10^6 per 10 cm plate for biochemical and immunoblotting assays. The cells were incubated for 24 h, treated with the indicated concentration of salirasib or with the vehicle (0.1% DMSO; control) for the times specified in each experiment, and then subjected to the various assays as described below. For 9L implantation, a pellet of 1×10^8 cells suspended in 2 mL PBS was prepared.

Salirasib Preparation

For *in vitro* experiments, salirasib and the control vehicle (0.1% DMSO) were prepared in DMEM at different concentrations, and each mixture was placed in the cell culture plates, so that the final concentrations of salirasib were 0, 6.25, 12.5, 25, 50, or 100 μmol/L, whereas the DMSO concentration was adjusted to 0.1%. Salirasib, a gift from Concordia Pharmaceuticals, was prepared as described previously (22).

For *in vivo* experiments, salirasib was dissolved in ethanol and the solution was alkalinized by the addition of 1 N NaOH and then diluted with PBS to obtain a solution of 3.0 mg/mL salirasib (pH 8.0; 1% ethanol). This solution was diluted to create a final concentration of 50 μmol/L salirasib in PBS containing 10% sucrose based on our previous experiments (12). For preparation of the control vehicle, we used ethanolic PBS without salirasib.

Cell Growth Assay

9L cells were treated with salirasib (6.25, 12.5, 25, 50, or 100 μmol/L) or DMSO (0.1%) for 5 days. The effect of salirasib on cell growth was determined by direct counting of cells collected from each well. To calculate the average percentage of viable cells (mean ± SD, $n = 4$), we divided the number of cells counted for each salirasib concentration by the number of cells in the control group. The experiment was down in quadruplicate.

GTPase Pull-down and Western Blotting Assays

9L cells were treated with salirasib (25 or 50 μmol/L) or DMSO (0.1%) for 24 h. The cells were then stimulated with epidermal growth factor (100 ng/mL; 5 min) and lysed. Lysates containing 1 mg protein were used to determine the Ras-GTP content by the glutathione *S*-transferase-RBD (Ras-binding domain of Raf) pull-down assay as described elsewhere (23). Total lysates and pull-down supernatants were subjected to SDS-PAGE and then immunoblotted with the following antibodies: anti-pan-Ras (1:2,500), anti-phospho-extracellular signal-regulated kinase (ERK; Thr^{183} and Tyr^{185}; 1:10,000), anti-ERK2 (1:1,000), and anti-β-tubulin (1:500). The immunoblots were exposed either to 1:2,500 peroxidase goat anti-mouse IgG or to 1:2,500 peroxidase goat anti-rabbit IgG, and protein bands were visualized by enhanced chemiluminescence and quantified by densitometry using EZQuant-Gel 2.1 software (EZQuant). Mouse anti-pan-Ras antibody (Ab-3) was from Calbiochem; mouse anti-phospho-ERK antibody and mouse anti-β-tubulin antibody were from Sigma-Aldrich; rabbit anti-ERK antibody was from Santa Cruz Biotechnology.

In vivo Experimental Design

A treatment solution containing salirasib and a control solution (without salirasib) were mixed with 10% sucrose (for increased efficacy) and with Gd-DTPA (1:70; for real-time imaging) and infused into the striatum of 9L gliosarcoma-bearing Fisher rats (males; 250-300 g) for the efficacy studies and into the striatum of normal Fisher rat brains for the toxicity studies.

For the efficacy studies, the extent of convection and the tumor volume at baseline were assessed by T_1- and T_2-weighted MRI acquired immediately after treatment. T_2-weighted and contrast-enhanced T_1-weighted MRI were acquired periodically thereafter to monitor tumor growth rate. The growth rate of treated rats relative to that of control rats as well as the correlation between extent of CED and tumor growth rate was studied as functions of time after treatment.

For the toxicity studies, the extent of convection was assessed by T_1-weighted MRI acquired immediately after treatment. Procedure-related toxicity (such as hydrocephalus caused by infusion into the ventricles) was assessed by T_2-weighted MRI acquired immediately after the treatment. Early and late tissue toxicity were assessed by T_2-weighted and diffusion-weighted images acquired 24 h and 2 weeks post-treatment (12). In addition, the rats' weight was monitored throughout the 2-week follow-up period.

Tumor Implantation

Male Fisher rats (250-300 g) were deeply anesthetized by i.m. injections of 600 μL of 22.5 mg/mL ketamine and 0.3% xylasine given twice in 15 min intervals. The striata of the rats were then inoculated with tumors as follows: the bregma was identified through a midline scalp incision, and a 1 mm burr hole was drilled in the right region of the skull, 3 mm anterior and 2 mm lateral to the bregma. A 33-gauge needle attached to a 1,000 μL syringe (Gastight; Hamilton) containing the 9L pellet was placed stereotactically in the striatum at a depth of 5.5 mm. Cells were infused with a syringe pump (Bee Hive; BASi) at a rate of 2 μL/min for 5 min, so that the final number of implanted cells was 5×10^5. The burr hole was then sealed with bone wax to prevent the tumor from growing out of the skull.

CED Procedure

In the 9L tumor-bearing rats, the burr hole that was drilled for cell implantation was reopened after 4 days and then used for CED treatment. In the rats treated for toxicity (normal rat brains), new burr holes were drilled as described above. Before infusion, Gd-DTPA was added to the salirasib or control solution to a concentration of 1:70. Salirasib or control solution was infused into the tumors for the efficacy studies or the striatum for the toxicity studies of deeply anesthetized rats for 40 min at a rate of 1 μL/min using the syringe pump described above. Both control and salirasib-treated rats were scanned immediately after treatment.

MRI Monitoring

The immediate formation and extent of CED as well as tumor follow-up were assessed with a General Electric 0.5 T interventional MRI machine [Signa SP/i (special proceeding/interventional)] equipped with the LX operating system and at a field-gradient intensity of up to 1 gauss/cm. The early and late toxicity, using diffusion-weighted MRI, were assessed with a General Electric 3.0 T MR system equipped with the HD 12x operating system and at a field-gradient intensity of up to 4 gauss/cm. Specially designed animal volume coils, 5 cm in diameter, were used for data acquisition.

T_2-weighted fast spin echo MRI were acquired with a 256×128 matrix, 12×9 cm^2 field of view, repetition time of 3,000 ms, echo time of 90 ms, and 3 mm slices with no gap. T_1-weighted images were acquired with a 256×128 matrix, 12×9 cm^2 field of view, repetition time = 400 ms, echo time = 12 ms, and 3 mm slices, no gap. Line-scan diffusion-weighted MRI were acquired with 256×128 matrix, 12×9 cm^2 field of view, repetition time = 5,440 ms, echo time = 142 ms, and 2 mm slices. Due to the limitation of the relatively thick (3 mm) slices on the 0.5 T system, each sequence was scanned twice, where the second time was acquired with a shift of 1.5 mm relative to the first, to enable maximum sensitivity to changes.

Calculation of Extent of CED

The gadolinium enhancement obtained from T_1-weighted MRI reflects the infusate distribution in the rat brain (12). Thus, the volume (in cm^3) of infusate distribution was calculated from the T_1-weighted MRI acquired immediately after CED treatment. Regions of interest were defined over the entire enhancing region in each slice (excluding the ventricles). Number of pixels in the regions of interest were counted and then multiplied by the volume of a single pixel as described earlier (12).

Calculation of Tumor Volume

The initial tumor volume (in cm^3) was calculated from T_2-weighted MRI, whereas the extent of CED was calculated from the contrast-enhanced T_1-weighted MRI at the same session for each rat. For the follow-up, rats were first injected (i.p) with 0.1 mL of 1 mmol/L Gd-DTPA then scanned. The volume of the tumor in these follow-ups was calculated from contrast-enhanced T_1- and T_2-weighted MRI. Regions of interest were defined over the entire enhancing region in each slice (excluding the ventricles). Numbers of pixels in the regions of interest were counted and then multiplied by the volume of a single pixel.

Calculation of Tumor Growth Rate

The tumor growth rate for each rat was calculated as the ratio between the tumor volume measured in a certain follow-up scan and the tumor volume measured in the first follow-up scan. The ratio was calculated for each follow-up scan. Average tumor growth ratios (mean ± SE) are presented for the salirasib (n = 13) and the control (n = 19) groups.

Correlation between CED Efficacy and Tumor Growth Rate

The correlation between CED efficacy and tumor growth rate was calculated by plotting the CED volume versus the growth rate for each rat. Correlations were calculated separately for growth rates between the second and first follow-up scans, the third and second follow-up scans, and the third and first follow-up scans.

Results

Salirasib Induces Growth Inhibition and Disruption of Ras Signaling in 9L Cells

Salirasib (farnesyl thiosalicylic acid) was designed as a small-molecule Ras inhibitor (22). With the aim of integrating salirasib into the CED model, we first examined its effect on the rat 9L gliosarcoma cell line as a brain tumor model. We did this by employing a simple cell growth assay in which 9L cells were treated with salirasib (6.25, 12.5, 25, 50, or 100 μmol/L) or, as a control, with DMSO (0.1%). Five days later, cells were collected and counted. Figure 1A and *B* show that salirasib induced a dose-dependent inhibition of 9L cell growth with an IC_{50} value of about 35 μmol/L. This concentration has been shown

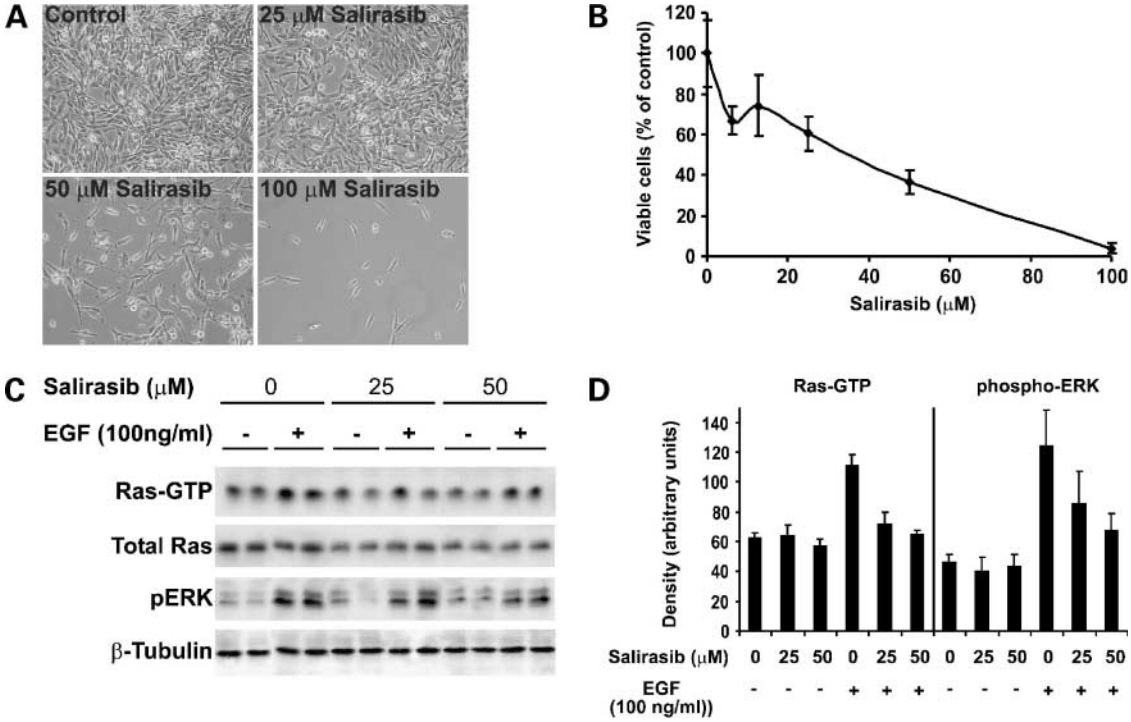

Figure 1. Salirasib inhibits cell growth and Ras signaling in rat 9L gliosarcoma cells. 9L cells were plated in 24-well plates at a density of 5,000 per well (for cell growth assays) or in 10 cm plates at a density of 1×10^6 per plate (for Ras signaling assays). After 24 h, the cells were treated with salirasib at the indicated concentrations or with a control vehicle (0.1% DMSO). For the cell growth assay, the cells were imaged, 5 d after treatment, using an Olympus fluorescence microscope (objective, ×10) and were then collected and counted. Typical images are shown in **A**. Mean ± SD numbers of live cells expressed as percentages of cells in the control solution ($n = 4$) are shown in **B**. For Ras signaling assays, cells in duplicate wells were serum starved for 12 h before being treated with epidermal growth factor for 5 min and then lysed. Ras, Ras-GTP, and phospho-ERK levels in the lysates were determined by Western immunoblotting and anti-Ras and anti-phospho-ERK antibodies as described in Materials and Methods. As a loading control, we used β-tubulin assayed with anti-β-tubulin antibody. Typical immunoblots of one of two experiments with similar results are shown in **C**. Densitometry of the immunoblots (mean ± SE; $n = 4$) is shown in **D**. *, $P < 0.05$; **, $P < 0.01$, epidermal growth factor-stimulated cells treated with salirasib versus untreated cells.

previously to be efficient in terms of growth inhibition in various human cancer cell lines (16, 24–27). Under the conditions employed here, cell death (indicated by Hoechst staining), both in the absence and in the presence of Salirasib, was lower than 10% (data not shown).

In addition, salirasib caused a dose-dependent decrease in the epidermal growth factor-stimulated increase in active, GTP-bound Ras as well as a decrease in total Ras (Fig. 1C and *D, left*). Salirasib (50 μmol/L) also caused a decrease in epidermal growth factor-stimulated Ras signaling to the Raf/MEK/ERK cascade as indicated by the observed decrease in phospho-ERK (Fig. 1C and *D, right*). These findings showed that salirasib acts as an effective Ras inhibitor in rat 9L gliosarcoma cells and therefore has an antiproliferative effect on these cells.

Extent of CED

The extent of convection was reflected by the T_1-weighted MRI acquired immediately after CED treatment with infusates mixed with Gd-DTPA (12). Poor convection was characterized by significant backflow along the catheter and into the ventricles depicted in the images as significant enhancement in the ventricles and little or no enhancement in the striatum (Fig. 2B). Efficient convection was reflected by significant spread into the striatum with minimal backflow into the ventricles (Fig. 2A). In some cases, owing to the characteristically dense tissue texture of massive 9L tumors, if a tumor had grown enough to form a mass at the time of CED treatment (shown in Fig. 2D), we found evidence of convection around the tumor but little or no penetration into the tumor itself (Fig. 2C).

Effect of Salirasib on Normal Rat Brain—Toxicity Study

Twelve naive rats were treated by CED of salirasib or the solvent. One of the rats died due to the surgical procedure. There were no other mortalities. The volume of distribution, as calculated from the immediate T_1-weighted MRI, was similar for the two groups: salirasib 60.3 ± 10.5 mm^3 ($n = 5$) and control 72.0 ± 19.1 mm^3 ($n = 6$); $P < 0.62$ (two-tailed Welch-corrected t test).

As shown in Fig. 3, no toxicity was observed in the MRI acquired for either the control or the salirasib-treated group compared with rats treated with carboplatin, which caused severe tissue damage (Fig. 3). During the first MRI follow-up, acquired 24 h post-treatment, 1 control rat showed mild edema in the striatum, which was resolved by the time of second follow-up, 2 weeks later. Two control rats and two salirasib-treated rats showed minor tissue damage at the needle entrance point. These abnormalities were resolved as well by the time of the second follow-up.

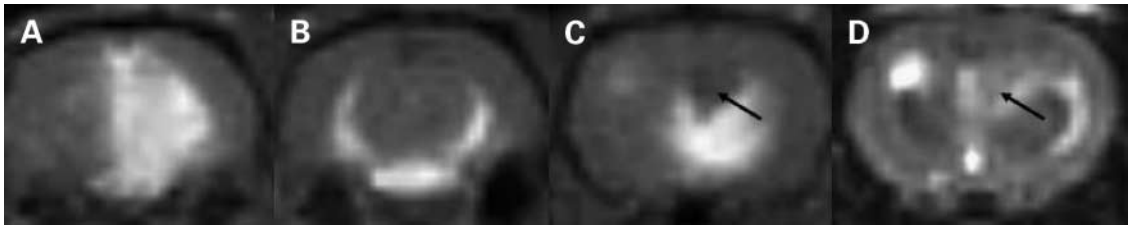

Figure 2. MRI of CED. Examples of axial T_1- or T_2-weighted MRI acquired immediately after CED. **A,** T_1-weighted MRI showing the contrast agent diffusing nicely throughout the implantation region, representing efficient delivery of salirasib. **B,** a T_1-weighted MRI showing a nonefficient convection reflected as complete backflow into the ventricular system. **C,** a T_1-weighted MRI showing the contrast agent concentrated around the tumor region (*arrow*; tumor appears dark in T_1). **D,** a T_2-weighted MRI reciprocal to that in **C** showing the tumor region of interest (*arrow*; tumor appears bright in T_2).

There were no differences in weight gain between the salirasib-treated group and the control group; 9.6 ± 1.4% and 10.5 ± 3.9% weight gain over the 2-week follow-up for salirasib or control rats respectively ($P < 0.84$, two-tailed Welch-corrected t test).

Correlation between CED Efficacy and Tumor Growth Rate

This experiment was done in three sessions. In each session, rats in the treated group (n = 10-12) were treated by CED of salirasib and rats in the control group (n = 10-12) were treated with the solvent. Both groups were monitored by MRI immediately after the treatment and periodically thereafter. CED volumes were calculated from the immediate T_1-weighted MRI, and tumor volumes were calculated from the T_2-weighted and contrast-enhanced T_1-weighted MRI. The results are presented in Table 1.

The correlation between tumor growth rate (calculated from the first follow-up) and CED volume was significant in two of the three sessions ($P < 0.05$; Table 1). Moreover, the correlation coefficient of the relationship between tumor growth rate and CED volume, r^2, was high in all three groups (Table 1). This suggests that more efficient CED is correlated with increased treatment effects. The correlation coefficient was highest for the group with the smallest initial tumor volume and lowest for the group with the largest initial tumor volume, suggesting that the treatment was more efficient for smaller tumors. In addition, the correlation between CED volume and tumor growth rate decreased with time (Fig. 4). For example, in the group with the smallest initial tumor volume, the correlation coefficient was high when tumor growth rate was measured between the second and the first follow-ups (r^2 = 0.989), lower when tumor growth rate was measured between the third and the first follow-ups (r^2 = 0.64) and flat when it was measured between the third and the second follow-ups (r^2 = 0.02). These results suggest that the treatment affected tumor growth rate only up to the second follow-up presumably due to the single-dose treatment.

Effect of CED of Salirasib on Tumor Growth Rate

Altogether, 30 9L tumor-bearing rats were treated with CED of salirasib and 32 9L tumor-bearing rats were treated with CED of the solvent (controls). Tumor volumes as a function of time were calculated from the follow-up MRI scans acquired up to 2 weeks after treatment. Because initial tumor volumes varied between the groups, tumor growth rates were normalized to the initial tumor volume.

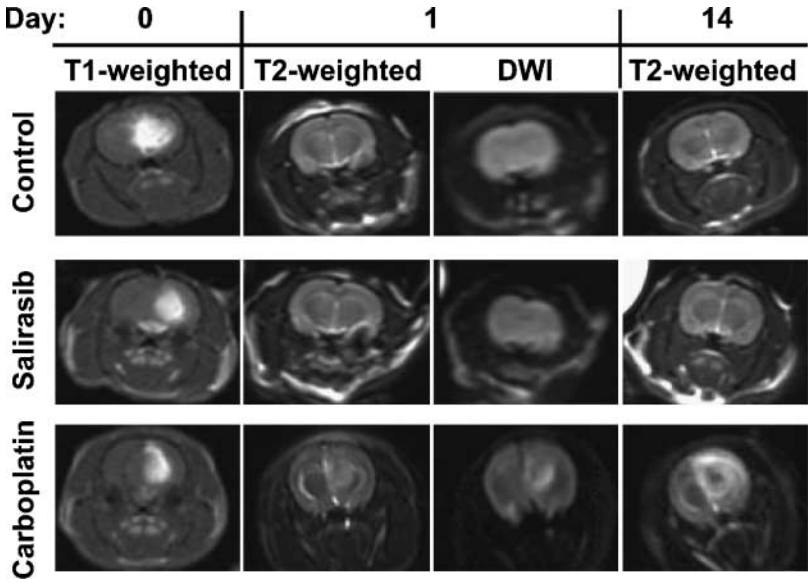

Figure 3. Lack of salirasib toxicity in normal brain tissue. Naive rats were convected either with vehicle control, 50 μmol/L Salirasib, or carboplatin (4 mg/mL), which was used as a positive control for toxicity. Typical T_1-weighted images depicting drug distribution taken immediately after CED (day 0) and typical T_2-weighted images and diffusion-weighted images taken on day 1 are shown. Also shown are typical T_2-weighted images taken 14 d after CED. The T_1-weighted images on day 0 show efficient CED in the various treatments. The T_2-weighted and diffusion-weighted images on day 1 show lack of early tissue toxicity in control and salirasib-treated rats compared with the carboplatin treated rat, which exhibited tissue damage in the form of edema and hydrocephalus. Late tissue toxicity (T_2, day 14) was observed only in the carboplatin-treated rat, which exhibited significant tissue necrosis and hydrocephalus.

Table 1. Correlation between tumor growth rate and CED volume

Treatment*	Initial tumor volume (cm^3)†	Correlation between growth rate and CED volume
Salirasib	20.27 ± 10.38	$r^2 = 0.989$; $P < 0.0005$
Control	19.09 ± 7.02	$r^2 = 0.189$; $P < 0.21$
Salirasib	51.59 ± 45.51	$r^2 = 0.745$; $P < 0.1369$
Control	25.42 ± 12.60	$r^2 = 0.0078$; $P < 0.868$
Salirasib	66.37 ± 51.10	$r^2 = 0.578$; $P < 0.017$
Control	50.25 ± 68.81	$r^2 = 0.11$; $P < 0.42$

NOTE: The correlation between tumor growth rate and CED volume is presented for three experiments. Growth rates correspond to the ratios of the tumor volumes at the second follow-up and the tumor volumes at the first follow-up for each animal (n = 5-8). These values were correlated with the CED volume of the corresponding animal using Pearson's correlation test. The r^2 values thus obtained are shown. P values indicate the statistical significance of the correlation. It can be seen that tumor growth rate is significantly affected by CED volume in the salirasib-treated rats and that this effect is larger for initially small tumors. The differences between initial tumor volumes of the groups reflect experimental variations among the randomly designated animals in each group.

*Treatment: 50 μmol/L salirasib or control vehicle.

†Initial tumor volume: calculated from the MRI (average ± SD).

In the salirasib-treated group, tumor growth was significantly slower for up to 2 weeks after treatment. Average tumor growth rates (normalized in each rat to the initial tumor volume and then averaged over the group of rats) were as follows: at 7 days, 1.15 ± 0.14 in salirasib-treated rats compared with 1.85 ± 0.22 in control ($P < 0.015$), and at 10 days, 1.61 ± 0.32 in salirasib-treated rats compared with 3.22 ± 0.55 in control ($P < 0.023$; Fig. 5A). At the last follow-up, the difference between the groups was not significant (1.87 ± 0.44 in salirasib-treated rats compared with 3.94 ± 0.75 in control; $P < 0.085$) probably because of the small number of surviving rats, which was also reflected by lack of difference in overall survival between the two groups. However, we found that in the surviving salirasib-treated rats the convection volumes were significantly higher (2.1 ± 0.25-fold) compared with the volumes of the nonsurviving rats (Fig. 5B). By contrast, in the control group, the convection volume ratio of surviving/nonsurviving rats was 1.3 ± 0.69, not significantly different than 1.0 (Fig. 5B). These results suggest that improved convection of salirasib correlates with increased survival rate.

Discussion

Glioblastomas are highly aggressive tumors for which there is no adequate treatment to date and are therefore associated with poor life expectancies where the median survival at 1 year is about 50% (28). Among other anomalies of gene expression, these tumors harbor a chronically activated Ras oncogene as a consequence of overexpression of growth factors and their receptors (29). Various attempts at Ras-directed therapy over the last decade have met with little success, leaving this therapeutic path wide open for novel agents (30). In this study, we employed the specific Ras inhibitor salirasib, which was originally designed to compete with Ras for its binding sites, thereby causing it to become dislodged from the cell membrane and subsequently undergo rapid degradation (19). Salirasib was shown previously to be highly potent in cell culture systems (24–27), in soft-agar assays (31, 32), and in various *in vivo* murine models (32–36). Promoter and biochemical analyses of glioblastoma cells treated with salirasib have disclosed that two important Ras-controlled transcription factors are down-regulated by the treatment. One is hypoxia-inducible factor-1, whose down-regulation leads to glycolysis shutdown (20), and the other is E2F1, whose down-regulation is associated with cell cycle arrest (21). In addition, salirasib, by inhibiting both anchorage-independent cell growth and cell migration, was shown to

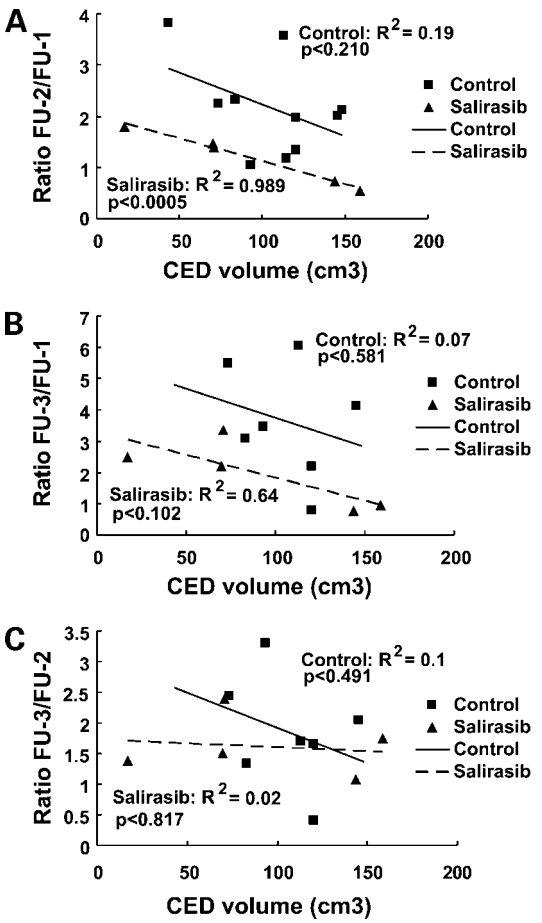

Figure 4. Effect of CED efficacy on tumor growth rate. Correlation between tumor growth rate (*Y* axis) and CED volume (*X* axis) is shown for the group with the smallest initial tumor volume. Tumor growth rate was calculated at several time points (follow-up, *FU*). The time intervals between 1st and 2nd, 2nd and 3rd and 3rd and 4th follow-ups were 3 d, 3 d, and 4 d, respectively. The correlation coefficient (r^2) was the highest for the tumor growth rate calculated between the second follow-up (*FU2*) and the first follow-up (*FU1*; **A**; $r^2 = 0.989$), lower for the rate between the third follow-up (*FU3*) and the first follow-up (**B**; $r^2 = 0.64$), and flat (**C**; $r^2 = 0.02$) for the rate between the third and the second follow-ups. The results suggest that the treatment affected tumor growth rate only up to the second follow-up.

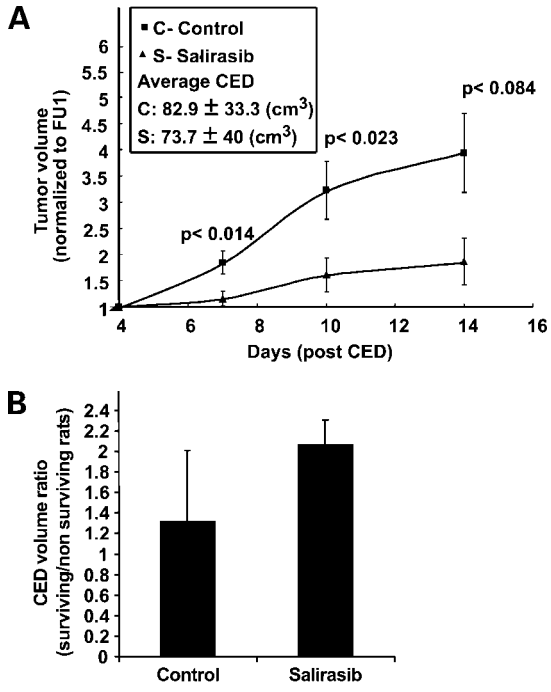

Figure 5. Effect of salirasib on tumor growth rate. **A,** average tumor growth rates (normalized in each rat to the initial tumor volume and then averaged over the group of rats) as a function of time after treatment for salirasib-treated rats and controls. Tumor growth rate was significantly slower in the salirasib-treated rat for up to 2 weeks after treatment. **B,** ratio between convection (CED) volumes in surviving and nonsurviving rats is shown for control and salirasib-treated rats (mean ± SD). The observed 2.1-fold increase in CED volume in the salirasib-treated group was highly significant ($P < 0.0017$, surviving rats versus nonsurviving rats in this group). In the control group, there was no significant difference (1.3-fold increase; $P < 0.128$).

avert the malignant phenotype of glioblastoma cells (16). These findings support the candidacy of salirasib as a potential therapy for glioblastoma multiforme. Salirasib is currently undergoing trials in patients with pancreatic cancer and with non-small cell lung cancer.[4]

In a study carried out by our group in a mouse model of head trauma (in which the blood-brain barrier is impaired), the highest concentrations of salirasib measured in brain homogenates from treated rats were of the order of 4.5 μmol/L (37). In the present study, the concentration of salirasib that was delivered directly into the tissue was 50 μmol/L, which is the concentration that was shown to effectively inhibit cell growth *in vitro* (Fig. 1).

Showing CED efficacy in a rat brain tumor model is hampered by the difficulty in simulating human brain tumor characteristics in means of tissue consistency and tumor infiltration. In humans, CED efficacy has been shown to vary among different drugs, from very high to very low response rates with various toxicity levels. In a previous publication, we have suggested that some of the differences between treatment effects obtained by different drugs may be explained by poor convection extent obtained with low viscosity infusates. Therefore, the main goal of the presented research was to show that salirasib can be efficiently distributed in a brain tumor model using a high-viscosity infusate and that treatment efficacy is increased with increased distribution volumes.

The results of this study show the significant efficacy of salirasib, administered via CED, in inhibiting tumor growth in a rat 9L tumor model. It is important to note that the present results were the outcome of a single CED treatment carried out soon after tumor implantation. In most animal models, it is practically impossible to repeat the CED treatment, because once the tumor becomes massive (detectable on MRI) drug penetration into the tumor becomes progressively more limited. This limitation can probably explain the lack of significant improvement in overall survival of the salirasib-treated rats (data not shown), although significant treatment effects were obtained from the overall tumor growth rates and the correlation with CED efficacy. In spite of the limitation, our results suggest that improvement in CED may allow its use also for large tumors and/or for high cellular density tumors. Indeed, we show that increased salirasib convection volumes correlate positively with survival (Fig. 5B).

Within each of the three sessions, the correlation between tumor growth rate and convection volume (drug distribution volume) was high, and in two of them, it was significant. This finding suggests that a more efficient CED is correlated with increased treatment effects and highlights the importance of achieving efficient convection of the drug within the tissue. Salirasib is normally dissolved in a low-viscosity solvent consisting of ethanolic PBS. In this study, we increased the viscosity of the solvent by adding 10% sucrose, thus enabling efficient CED, as discussed in our previous work (12).

The correlation coefficient was highest for the group with the smallest initial tumor volume and lowest for the group with the largest initial tumor volume, suggesting that the treatment was more efficient in smaller tumors. This phenomenon might be explained in terms of the texture of the 9L tumors; once they grow large enough to be imaged by MRI, they can no longer be efficiently penetrated by convection. An example is shown in Fig. 2C and *D*, where the delivered drug was adequately distributed by convection around the tumor, but no penetration was detectable.

The correlation between tumor growth and CED volume (efficacy) decreased with time after treatment in all three sessions as shown in Fig. 4. This effect is presumably attributable to the fact that the delivered drug was unable to penetrate to the full depth of the tumor, with resulting occurrence of residual tumor growth. As mentioned before, these tumors do not simulate well clinical tumors; therefore, the main goal of the study was to show significant treatment effect and its dependence on CED efficacy rather than improved overall survival.

[4] http://www.concordiapharma.com

In summary, the results of this study show, both *in vitro* and *in vivo*, the efficacy of salirasib in the treatment of brain tumors in a glioma rat model. In addition, the present results emphasize the importance of achieving efficient convection to maximize treatment efficacy. Our findings also highlight the importance of delivering drug concentrations high enough to serve as therapeutic doses not achievable by i.v. administration.

A unique characteristic of salirasib is its remarkable specificity for tumor tissue, which makes it an optimal drug for CED. We have observed no toxicity in either our *in vitro* or our *in vivo* studies (Figs. 1 and 3) despite the fact that the concentrations used in this work were at least an order of magnitude higher than previously reported salirasib concentrations detected in the brain (37).

Disclosure of Potential Conflicts of Interest

No potential conflicts of interest were disclosed.

Acknowledgments

We thank Shirley Smith for editorial assistance and Sharona Salomon for significant help in growing the 9L cells and assisting in tumor implantation and treatment procedures.

References

1. Rosenberg GA, Kyner WT, Estrada E. Bulk flow of brain interstitial fluid under normal and hyperosmolar conditions. Am J Physiol 1980;238: F42 – 9.

2. Reulen HJ, Graham R, Spatz M, Klatzo I. Role of pressure gradients and bulk flow in dynamics of vasogenic brain edema. J Neurosurg 1977;46: 24 – 35.

3. Ohata K, Marmarou A. Clearance of brain edema and macromolecules through the cortical extracellular space. J Neurosurg 1992;77:387 – 96.

4. Lieberman DM, Laske DW, Morrison PF, Bankiewicz KS, Oldfield EH. Convection-enhanced distribution of large molecules in gray matter during interstitial drug infusion. J Neurosurg 1995;82:1021 – 9.

5. Bobo RH, Laske DW, Akbasak A, Morrison PF, Dedrick RL, Oldfield EH. Convection-enhanced delivery of macromolecules in the brain. Proc Natl Acad Sci U S A 1994;91:2076 – 80.

6. Morrison PF, Laske DW, Bobo H, Oldfield EH, Dedrick RL. High-flow microinfusion: tissue penetration and pharmacodynamics. Am J Physiol 1994;266:R292 – 305.

7. Lidar Z, Mardor Y, Jonas T, et al. Convection-enhanced delivery of paclitaxel for the treatment of recurrent malignant glioma: a phase I/II clinical study. J Neurosurg 2004;100:472 – 9.

8. Weaver M, Laske DW. Transferrin receptor ligand-targeted toxin conjugate (Tf-CRM107) for therapy of malignant gliomas. J Neurooncol 2003;65:3 – 13.

9. Sampson JH, Akabani G, Archer GE, et al. Progress report of a phase I study of the intracerebral microinfusion of a recombinant chimeric protein composed of transforming growth factor (TGF)-α and a mutated form of the *Pseudomonas* exotoxin termed PE-38 (TP-38) for the treatment of malignant brain tumors. J Neurooncol 2003;65:27 – 35.

10. Kawakami M, Kawakami K, Puri RK. Interleukin-4-*Pseudomonas* exotoxin chimeric fusion protein for malignant glioma therapy. J Neurooncol 2003;65:15 – 25.

11. Husain SR, Puri RK. Interleukin-13 receptor-directed cytotoxin for malignant glioma therapy: from bench to bedside. J Neurooncol 2003;65: 37 – 48.

12. Mardor Y, Rahav O, Zauberman Y, et al. Convection-enhanced drug delivery: increased efficacy and magnetic resonance image monitoring. Cancer Res 2005;65:6858 – 63.

13. Boguski MS, McCormick F. Proteins regulating Ras and its relatives. Nature 1993;366:643 – 54.

14. Walsh AB, Bar-Sagi D. Differential activation of the Rac pathway by Ha-Ras and K-Ras. J Biol Chem 2001;276:15609 – 15.

15. Joneson T, White MA, Wigler MH, Bar Sagi D. Stimulation of membrane ruffling and MAP kinase activation by distinct effectors of RAS. Science 1996;271:810 – 2.

16. Goldberg L, Kloog Y. A Ras inhibitor tilts the balance between Rac and Rho and blocks phosphatidylinositol 3-kinase-dependent glioblastoma cell migration. Cancer Res 2006;66:11709 – 17.

17. Downward J. Ras signalling and apoptosis. Curr Opin Genet Dev 1998;8:49 – 54.

18. McCormick F. Signal transduction. How receptors turn Ras on. Nature 1993;363:15 – 6.

19. Haklai R, Gana-Weisz M, Elad G, et al. Dislodgment and accelerated degradation of Ras. Biochemistry 1998;37:1306 – 14.

20. Blum R, Jacob-Hirsch J, Amariglio N, Rechavi G, Kloog Y. Ras inhibition in glioblastoma down-regulates hypoxia-inducible factor-1α, causing glycolysis shutdown and cell death. Cancer Res 2005;65: 999 – 1006.

21. Blum R, Nakdimon I, Goldberg L, et al. E2F1 identified by promoter and biochemical analysis as a central target of glioblastoma cell-cycle arrest in response to Ras inhibition. Int J Cancer 2006;119: 527 – 38.

22. Marciano D, Ben-Baruch G, Marom M, Egozi Y, Haklai R, Kloog Y. Farnesyl derivatives of rigid carboxylic acids—inhibitors of ras-dependent cell growth. J Med Chem 1995;38:1267 – 72.

23. de Rooij J, Bos JL. Minimal Ras-binding domain of Raf1 can be used as an activation-specific probe for Ras. Oncogene 1997;14:623 – 5.

24. Zundelevich A, Elad-Sfadia G, Haklai R, Kloog Y. Suppression of lung cancer tumor growth in a nude mouse model by the Ras inhibitor salirasib (farnesylthiosalicylic acid). Mol Cancer Ther 2007;6:1765 – 73.

25. Yaari S, Jacob-Hirsch J, Amariglio N, Haklai R, Rechavi G, Kloog Y. Disruption of cooperation between Ras and MycN in human neuroblastoma cells promotes growth arrest. Clin Cancer Res 2005;11:4321 – 30.

26. Barkan B, Starinsky S, Friedman E, Stein R, Kloog Y. The Ras inhibitor farnesylthiosalicylic acid as a potential therapy for neurofibromatosis type 1. Clin Cancer Res 2006;12:5533 – 42.

27. Gana-Weisz M, Halaschek-Wiener J, Jansen B, Elad G, Haklai R, Kloog Y. The Ras inhibitor *S-trans,trans*-farnesylthiosalicylic acid chemosensitizes human tumor cells without causing resistance. Clin Cancer Res 2002;8:555 – 65.

28. Markert J. Glioblastoma multiforme: introduction. Cancer J 2003; 9:148.

29. Guha A, Feldkamp MM, Lau N, Boss G, Pawson A. Proliferation of human malignant astrocytomas is dependent on Ras activation. Oncogene 1997;15:2755 – 65.

30. Blum R, Kloog Y. Tailoring Ras-pathway-inhibitor combinations for cancer therapy. Drug Resist Updat 2005;8:369 – 80.

31. Weisz OA, Schnaar RL. Hepatocyte adhesion to carbohydrate-derivatized surfaces. II. Regulation of cytoskeletal organization and cell morphology. J Cell Biol 1991;115:495 – 504.

32. Egozi Y, Weisz B, Gana-Weisz M, Ben-Baruch G, Kloog Y. Growth inhibition of ras-dependent tumors in nude mice by a potent ras-dislodging antagonist. Int J Cancer 1999;80:911 – 8.

33. Jansen B, Schlagbauer-Wadl H, Kahr H, et al. Novel Ras antagonist blocks human melanoma growth. Proc Natl Acad Sci U S A 1999;96: 14019 – 24.

34. Weisz B, Giehl K, Gana-Weisz M, et al. A new functional Ras antagonist inhibits human pancreatic tumor growth in nude mice. Oncogene 1999;18:2579 – 88.

35. Jansen B, Heere-Ress E, Schlagbauer-Wadl H, et al. Farnesylthiosalicylic acid inhibits the growth of human Merkel cell carcinoma in SCID mice. J Mol Med 1999;77:792 – 7.

36. Haklai R, Elad-Sfadia G, Egozi Y, Kloog Y. Orally administered FTS (salirasib) inhibits human pancreatic tumor growth in nude mice. Cancer Chemother Pharmacol 2008;61:89 – 96.

37. Shohami E, Yatsiv I, Alexandrovich A, et al. The Ras inhibitor *S-trans,trans*-farnesylthiosalicylic acid exerts long-lasting neuroprotection in a mouse closed head injury model. J Cereb Blood Flow Metab 2003;23: 728 – 38.

Molecular Cancer Therapeutics

Salirasib (farnesyl thiosalicylic acid) for brain tumor treatment: a convection-enhanced drug delivery study in rats

Liat Goldberg, Aharon Ocherashvilli, Dianne Daniels, et al.

Mol Cancer Ther 2008;7:3609-3616.